Journal of Ethnopharmacology 337 (2025) 118882

Contents lists available at ScienceDirect

Journal of Ethnopharmacology

journal homepage: www.elsevier.com/locate/jethpharm

Investigation of the anti-inflammatory, anti-pruritic, and analgesic effects of sophocarpine inhibiting TRP channels in a mouse model of inflammatory itch and pain

Hekun Zeng [a], Zhe Zhang [a], Dan Zhou [a], Ranjing Wang [a], Alexei Verkhratsky [b,c,d], Hong Nie [a,*]

[a] State Key Laboratory of Bioactive Molecules and Druggability Assessment, Guangdong Province Key Laboratory of Pharmacodynamic Constituents of TCM and New Drugs Research, International Cooperative Laboratory of Traditional Chinese Medicine Modernization and Innovative Drug Development of Ministry of Education (MOE) of China, College of Pharmacy, Jinan University, Guangzhou, Guangdong, 510632, China
[b] Faculty of Biology, Medicine and Health, The University of Manchester, Manchester, United Kingdom
[c] Achucarro Centre for Neuroscience, IKERBASQUE, Basque Foundation for Science, Bilbao, Spain
[d] Department of Stem Cell Biology, State Research Institute Centre for Innovative Medicine, LT-01102, Vilnius, Lithuania

ARTICLE INFO

Handling Editor: dr. P Fernandes

Keywords:
Sophocarpine
Anti-inflammatory
Anti-pruritic
Analgesic
TRPA1
TRPV1

ABSTRACT

Ethnopharmacological relevance: Sophocarpine is a bioactive compound extracted from the dried root of *Sophorae Flavesentis* Aiton, a plant that has been used for thousands of years for various conditions including skin itch and pain. Its antipruritic and analgesic effects are suggested in publications, while the molecular mechanisms underneath interacting with TRP channels are not understood.

Aim of the study: We investigated the anti-inflammatory, antipruritic, and analgesic effects of sophocarpine in a murine inflammatory itch and pain model to elucidate the underlying mechanisms.

Materials and methods: We evaluated sophocarpine's anti-pruritic and analgesic effects by monitoring mice's scratching and wiping behaviors, and the anti-inflammatory effect by measuring psoriasis area and severity index (PASI) score. The mRNA and protein expression of TRPA1/TRPV1 was analyzed by real-time quantitative polymerase chain reaction and western blotting. We further investigated the relationship between sophocarpine and TRPA1/TRPV1 in mice administered allyl-isothiocyanate (AITC) or capsaicin and by molecular docking.

Results: We found that sophocarpine decreased scratching bouts, wipes, and the PASI score, reduced the TNF-α and IL-1β in the skin and TRPA1 and TRPV1 in the trigeminal ganglion. Pretreatment of sophocarpine decreased AITC-induced scratching bouts and wipes and capsaicin-induced wipes. We also found potential competitive bindings between sophocarpine and AITC/capsaicin to TRPA1/TRPV1.

Conclusions: Sophocarpine is a potential competitive inhibitor of TRPA1 and TRPV1 channels eliciting strong anti-inflammatory, anti-pruritic, and analgesic effects, suggesting its significant therapeutic potential in treating diseases with inflammatory itch and pain.

1. Introduction

Itch is an unpleasant sensation that causes the need to scratch the affected area to remove puritogens thus providing temporary relief (Dhand and Aminoff, 2014). Differing from the itch, pain-related harm detection instigates acute withdrawal or other protective behaviors. Both itch and pain are distinct sensations relying on interacting sensory subdivisions; however, opioids could inhibit pain but generate itch that indicates distinct underlying mechanisms (Miyamoto and Patapoutian, 2011).

Chronic itch and pain have broadly overlapping mediators and functions (Li et al., 2021). For example, nerve growth factor could induce primary afferents sensitization in both chronic itch and pain (Yamaguchi et al., 2009). Finding effective medicine targeting the common mechanism to relieve itch and pain is required to avoid physical or mental issues brought by both uncomfortable sensations coexisting.

In humans, the transient receptor potential (TRP) channels family

* Corresponding author.
E-mail addresses: lyncus.zeng@foxmail.com (H. Zeng), 1191428423@qq.com (Z. Zhang), 1690507398@qq.com (D. Zhou), alexej.verkhratsky@manchester.ac.uk (A. Verkhratsky), hongnie1970@163.com (H. Nie).

https://doi.org/10.1016/j.jep.2024.118882
Received 5 August 2024; Received in revised form 25 September 2024; Accepted 30 September 2024
Available online 2 October 2024

covers 27 members classified into six groups of TRPC (canonical), TRPV (vanilloid), TRPM (melastatin), TRPP (polycystin), TRPML (mucolipin), and TRPA (ankyrin); an additional group of TRPN (NompC-like) is present in invertebrates and fishes. The TRP channels are widely expressed throughout the nervous system and contribute to all types of sensing including thermal sensation, nociception, chemisorption, equilibrioception, and taste (Nilius and Owsianik, 2011). The TRP channels are archetypal cationic channels, and many are highly permeable to Ca^{2+} ions (Tsagareli and Nozadze, 2020). The TRPA1 and TRPV1 subfamilies contribute to both inflammatory itch and pain sensation (Landini et al., 2022; Moore et al., 2018). Many pro-inflammatory mediators such as bradykinin, leukotrienes, tumor necrosis factor-α (TNF-α), and interleukin-1β (IL-1β) can activate the TRPA1 and TRPV1 channels to mediate pain (Basbaum et al., 2009). In addition, TRPA1 was suggested to mediate histamine-independent itch, whereas TRPV1 mediates histamine-dependent itch (Shim et al., 2007; Wilson et al., 2011).

Sophorae Flavesentis Radix (SFR, Kushen in Pinyin), the dried root of *Sophorae Flavesentis* Aiton (plant name has been checked with http s://www.worldfloraonline.org/, accessed August 10, 2024), is a Traditional Chinese Medicine used to relieve itch and pain for thousands of years. The traditional antipruritic effect of SFR is documented in The Pharmacopoeia of the People's Republic of China (Commission, 2020), and the amelioration of various cancer-related bone pain is summarized in a systematic review of the clinical use of the compound Kushen injection, where SFR(Kushen) is the main ingredient (PROSPERO ID : CRD42022361349) (Li et al., 2023). In our previous study, cell membrane immobilized chromatography screened out sophocarpine as an active compound that could bind to receptors on the plasma membrane of cells in dorsal root ganglion (DRG) (Zhang et al., 2021). The antinociceptive and anti-inflammatory effect of sophocarpine is proved in thermally and chemically induced pain models (Gao et al., 2009), and the antipruritic effect is predicted in network pharmacological analysis of Run-zao-zhiyang Capsule (Wang et al., 2023), while the mechanism underneath the antinociceptive and antipruritic effect of sophocarpine on TRP channels in DRG or trigeminal ganglion (TG) is yet to carry out. This study employed a mouse model of allergic contact dermatitis (ACD), manifesting inflammatory itch and pain. We investigated the anti-inflammatory, analgesic and anti-pruritic effects of sophocarpine, and its potential action mechanism in vivo. We further used the agonists of TRPA1/TRPV1 to discuss the relationship between sophocarpine and TRPA1/TRPV1 in vivo and silico.

2. Materials and methods

2.1. Chemicals and reagents

For animal experiments: Squaric acid dibutylester (SADBE, >97% purity, D2203) was obtained from Tokyo Chemical Inc. (Tokyo, Japan). Sophocarpine (98%, CN010535) was obtained from Chengdu Push Biotechnology Co., Ltd. (Chengdu, China). Capsazepine (99.66% purity, S813702) was obtained from Selleck Chemicals LLC (Houston, TX, USA). Dexamethasone (98% purity, D829854) was obtained from Shanghai Macklin Biochemical Co., Ltd. (Shanghai, China). Capsaicin (98% purity, A-JN938) and allyl isothiocyanate (AITC) (94% purity, AV725) was obtained from 9 Ding Chemistry (Shanghai) Co. Ltd. (Shanghai, China). Acetone (>99.5% purity, HB02) was obtained from Guangzhou Chemical Reagent Factory (Guangzhou, China). Tween-80 (P4780) was obtained from Sigma-Aldrich Co. (MO, USA). For RT-qPCR experiments: TRIzol reagents (Invitrogen) (15596026) were obtained from ThermoFisher Scientific (Waltham, MA, USA) to extract total mRNA from the sample. Prime Script RT reagent kit with gDNA Eraser (RR047B) and TB Green Premix Ex Taq II (Tli RNase H Plus) (RR82WR) was obtained from Takara Bio Inc. (Tokyo, Japan) to synthase complementary DNA (cDNA) and amplify cDNA, respectively. For western blotting experiments: Cell lysis buffer for Western and IP (P0013) and SDS-PAGE Gel Preparation Kit (P0012AC) was obtained from Beyotime Biotech Inc. (Shanghai, China) to prepare protein samples and 15% SDS-PAGE gel, respectively. Polyvinylidene difluoride (PVDF) membrane (1620177) was obtained from Bio-Rad Laboratories, Inc. (CA, USA) for protein blotting. Tris-buffered saline with 0.1% Tween® 20 Detergent (TBST, T1082) was obtained from Beijing Solarbio Science & Technology Co., Ltd. (Beijing, China) for PVDF membrane wash. Rabbit polyclonal anti-mouse primary antibodies against TRPV1 (NBP1-97417) and TRPA1 (NB100-98841) were obtained from Novus Biologicals, LLC. (Littleton, CO, USA) and those against TNF-α (Ab6671) and IL-1β (Ab9722) were obtained from Abcam Ltd. (Cambridge, UK), and mouse monoclonal anti-mouse primary antibody against β-actin was obtained from Cell Signaling Technology, Inc. (Danvers, MA, USA) for specific protein binding. Horseradish peroxidase-conjugated goat anti-rabbit secondary antibody (A0208) and goat anti-mouse secondary antibody (A0216) were obtained from Beyotime Biotech Inc. (Shanghai, China) for antibody binding. Super ECL detection reagent (P1010) was obtained from Applygen Technologies Inc. (Beijing, China) for the antibody detection. X-ray film (XBT-1) was obtained from Carestream Health, Inc. (NY, USA) for imaging.

2.2. Animals

Male mice (6-week-old, 20 ± 2 g) were purchased from the SPF (Beijing) Biotechnology Co. Ltd. (Certificate NO. SCXK (Beijing) 2016-0002). All mice were housed under a cycle of 12 h light/dark and given standard laboratory food and tap water in the Jinan University Medical School's Laboratory Animal Management Center and (Certificate No. SYXK (Guangdong) 2017-0174). All experimental procedures and animal welfare strictly followed the Guide for the Care and Use of Laboratory Animals and related to Jinan University's ethical regulations following the Guidelines for the Ethical Review of Laboratory Animal Welfare (GB/T 35892-2018), and approved by the Laboratory Animal Welfare and Ethics Committee of Jinan University (IACUC-20180621-07, 19 September 2023).

2.3. Establishment of allergic contact dermatitis mouse model and drug administration

The ACD or Contact Hypersensitivity (CHS) mouse model was established as described by applying SADBE dissolved in acetone on the right cheek (Xu et al., 2018) (Fig. 1). Briefly, the mice's abdomen was shaved on Day −1. Starting from Day 1, 25 μL 1% SADBE (v/v) was applied to the abdominal shaved area for three consecutive days once daily. The mice's right cheek was shaved on Day 6, and 25 μL 1% SADBE was applied to the cheek shaved area once daily for three consecutive days starting from Day 8 to excite the ACD. The control group was treated with 25 μL pure acetone instead of 1% SADBE.

70 C57BL/6 mice were randomly allocated into 7 groups: control group, ACD group, dexamethasone group, capsazepine group, 10 mg/kg sophocarpine group, 30 mg/kg sophocarpine group and 60 mg/kg sophocarpine group. Three doses of sophocarpine (60, 30, and 10 mg/kg), capsazepine (30 mg/kg), dexamethasone (5 mg/kg) and saline were administrated intragastrically (i.g.) through iron catheters on Day 11 (24 h after the third application of 1% SADBE on the cheek) (Fig. 1).

2.4. Evaluation of spontaneous scratching and wiping behaviors

To evaluate the spontaneous scratching and wiping behavior, mice were placed in a separate, clear plastic container in 9 × 9 × 13 cm3 with a small amount of bedding inside, and a camcorder was positioned above the container to record two mice at a time for 2 h, at 1 h after drug administration. Four mirrors were placed with their bottoms aligned to the 4 lines of the square bottom of each container, to give views of the mice from all 4 sides. Mice were trained for 2 h daily from Day 1 to Day 10 and were placed into the container 30 min before video recording to

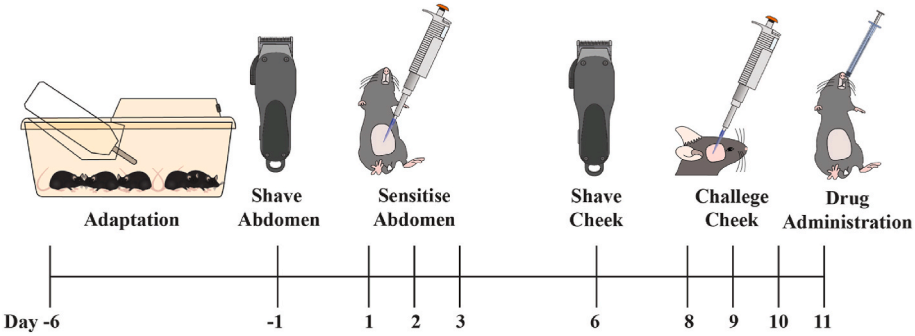

Fig. 1. The establishment of the ACD model on the cheek and intragastric drug administration. The shaved area is roughly 1.5 × 1.5 cm^2 in the abdomen and 0.8 × 0.8 cm^2 in the cheek.

let the mice get used to the surroundings. For each 2-h video, the itch-like scratching with the hindlimb and pain-like wiping with the forelimb was counted by an investigator blinded to the experimental design (Friedman et al., 2002; Shimada and LaMotte, 2008).

2.5. PASI scoring and measurement of skin-fold thickness

The image of each mouse's cheek skin was taken under brief anesthesia after the video recording. The severity of the inflammation was rated for the amount of erythema, thickening, and scaling, each assessed independently on the following scale: 0, none; 1, slight; 2, moderate; 3, marked; and 4, very marked. The PASI score was calculated as the sum of the erythema, scaling, and thickening scores. The cheek fold thickness of each mouse was measured 3 times using a micrometer (Mitutoyo, Tokyo, Japan), and the mean was calculated.

2.6. Real-time quantitative polymerase chain reaction (RT-qPCR)

After the PASI scoring described above, mice were sacrificed and the trigeminal ganglion (TG) from the treated side was immediately isolated. The mRNA was extracted and cDNA was synthesized from 100 μg of total RNA. Each cDNA sample was amplified for the gene of interest and β-actin in a 15 μL reaction volume. The PCR conditions were 95 °C for 30 s, 40 cycles of 95 °C for 5 s, and 60 °C for 60 s. The whole procedure was performed according to the manufacturer's instructions. The mRNA levels of all genes were normalized to the measured mRNA values of the housekeeping gene β-actin. The primers used are listed in Table 1.

2.7. Western blotting

The sample was isolated as described in the previous section. The total protein was extracted and 30 μg of each sample was added to 15% SDS-PAGE gel prepared. Protein separation was performed at room temperature with 90 V for 30 min followed by 120 V for 60 min, and protein transferring to the PVDF membrane was performed on ice with a current of 250 mA for 1.5 h. Afterward, the PVDF membrane was washed 6 times with TBST for 5 min each and blocked with 5% skim milk powder for 60 min on a shaking table at room temperature. The PVDF membrane was cut into strips between 110 and 70 kDa for TRPA1 and TRPV1 primary antibody incubation, between 55-40 kDa and 40-35 kDa for β-actin, and between 25 and 15 kDa for TNF-α and IL-1β, to avoid unknown protein loss by using stripping buffer. Membrane strips were washed with TBST and incubated with primary antibodies respectively at 4 °C overnight. After washing with TBST, PVDF membrane strips were incubated with HRP-conjugated secondary antibodies for 2 h on the shaking table at room temperature. After washing with TBST, the detection was performed with the Super ECL detection reagent and X-ray film or AI600 Imager (GE, Buckinghamshire, UK).

Table 1
Primer sequences.

Genes	Primer sequences
TNF-α-Forward	5'-TCTACTGAACTTCGGGGTGATCG-3'
TNF-α-Reverse	5'-ACGTGGGCTACAGGCTTGTCA-3'
IL-1β-Forward	5'-CCTTGTGCAAGTGTCTGAAGCAGC-3'
IL-1β-Reverse	5'- GCCACAGCTTCTCCACAGCCA-3'
TRPV1-Forward	5'-ATCTTCACCACGGCTGCTTACT-3'
TRPV1-Reverse	5'-CACAAACAAACTCTTGAGGGATG-3'
TRPA1-Forward	5'-AATCTCTGTCCTCTGCATCACG-3'
TRPA1-Reverse	5'-ACAATGCAGTGGGGTATTTCC-3'
β-actin-Forward	5'-AGATGTGGATCAGCAAGCAGG-3'
β-actin-Reverse	5'-GCTCAGTAACAGTCCGCCTAGA-3'

2.8. Capsaicin and AITC-induced behavioral testing

50 C57BL/6 mice were randomly allocated into 5 groups: Control group, AITC group, AITC + sophocarpine group, capsaicin group, and capsaicin + sophocarpine group, in capsaicin and AITC-induced behavior testing. The 10 mg/kg sophocarpine or the same volume of saline was administrated intragastrically (i.g.) for the capsaicin + sophocarpine and AITC + sophocarpine group or other groups at 1 h before capsaicin and AITC, respectively. After adaptation for 30 min, 1 mg/kg capsaicin (w/v, dissolved in 7% Tween-80), 1% AITC (v/v, diluted in 7% Tween-80), and 10 μL 7% Tween-80 as the vehicle was intradermally administrated into mice cheek of capsaicin groups, AITC groups and control group respectively. In this assay, the video was recorded for 30 min following capsaicin and AITC injection. The pain-like behavior and itch-like behavior were measured as described in 2.4.

2.9. Molecular docking

The AutoDock Vina plugin in Chimera, and ChimeraX were used for molecular docking simulations and visualization of sophocarpine, capsaicin, and AITC into active binding sites of TRPA1 and TRPV1. The molecular structure of sophocarpine (ZINC3881784), capsaicin (ZINC1530575), capsazepine (ZINC3871859), AITC (ZINC1687017), and HC-030031 (ZINC898145) was adopted from ZINC (https://cartblanche22.docking.org). (Tingle et al., 2023) The protein structure of TRPV1 (PDB ID: 3J5P) and TRPA1 (PDB ID: 3J9P) was adopted from RCSB Protein Data Bank (https://www.rcsb.org/) (Burley et al., 2023). Autodock Vina 1.1.2 in UCSF Chimera 1.17.3 was used for molecules and proteins preprocessing, docking box determination and docking simulations, according to a similar tutorial on https://vina.scripps.edu/ (Pettersen et al., 2004; Trott and Olson, 2010). The docking results were visualized, and atomic distances of hydrogen bonds were measured by ChimeraX 1.6.1 (Pettersen et al., 2021).

2.10. Statistical analysis

All the data are shown as mean ± S.E.M. All western blot images

were analyzed by ImageJ (NIH, Maryland, USA), and representative pictures were arranged and adjusted with Adobe Illustrator only for better demonstration. All statistical analyses and figure processing were performed using GraphPad Prism 9 (GraphPad Software, La Jolla, CA, USA). The comparisons of quantitative data among groups were performed using one-way ANOVA, followed by Bonferroni corrections for testing between individual means. A value of $p < 0.05$ was considered statistically significant.

3. Results

3.1. Sophocarpine reduced scratching and wiping behaviors, and skinfold thickness in ACD mice

Mice in the ACD group exhibited significantly more scratching bouts and wipes than in the control group (Fig. 2a-b). Compared with the ACD group, mice in the dexamethasone, capsazepine, and all sophocarpine groups exhibited fewer scratching bouts, while only the sophocarpine groups exhibited fewer wipes (Fig. 2a-b). Sophocarpine reduced mice wiping behavior in a dose-dependent manner, whereas 60 mg/kg and 30 mg/kg sophocarpine showed the same potency against scratching behavior, having a stronger effect than 10 mg/kg sophocarpine (Fig. 2a-b). The skinfold thickness of the dexamethasone group, 30 mg/kg sophocarpine group, and 10 mg/kg sophocarpine group was lower than that of the ACD group. There was no difference between the capsazepine group, 60 mg/kg sophocarpine group and the ACD group (Fig. 2c).

3.2. Sophocarpine improved the cheek skin inflammation in SADBE-induced ACD mice

In the control group, we found no visual indications of redness, scaling, or swelling of the cheek skin (Fig. 2d). The ACD group demonstrated noticeable scaling, swelling, and redness (Fig. 2d). Further study showed that the dexamethasone and sophocarpine groups had significantly lower PASI scores than the ACD group (Fig. 2e). In the detailed scoring of the PASI scale, there was no difference between the dexamethasone group, all sophocarpine groups, and the ACD group in erythema scoring; the dexamethasone group and 60 mg/kg sophocarpine group scored lower in scaling score; and all groups scored lower in thickening score compared with those of the ACD group (Fig. 2f-1h).

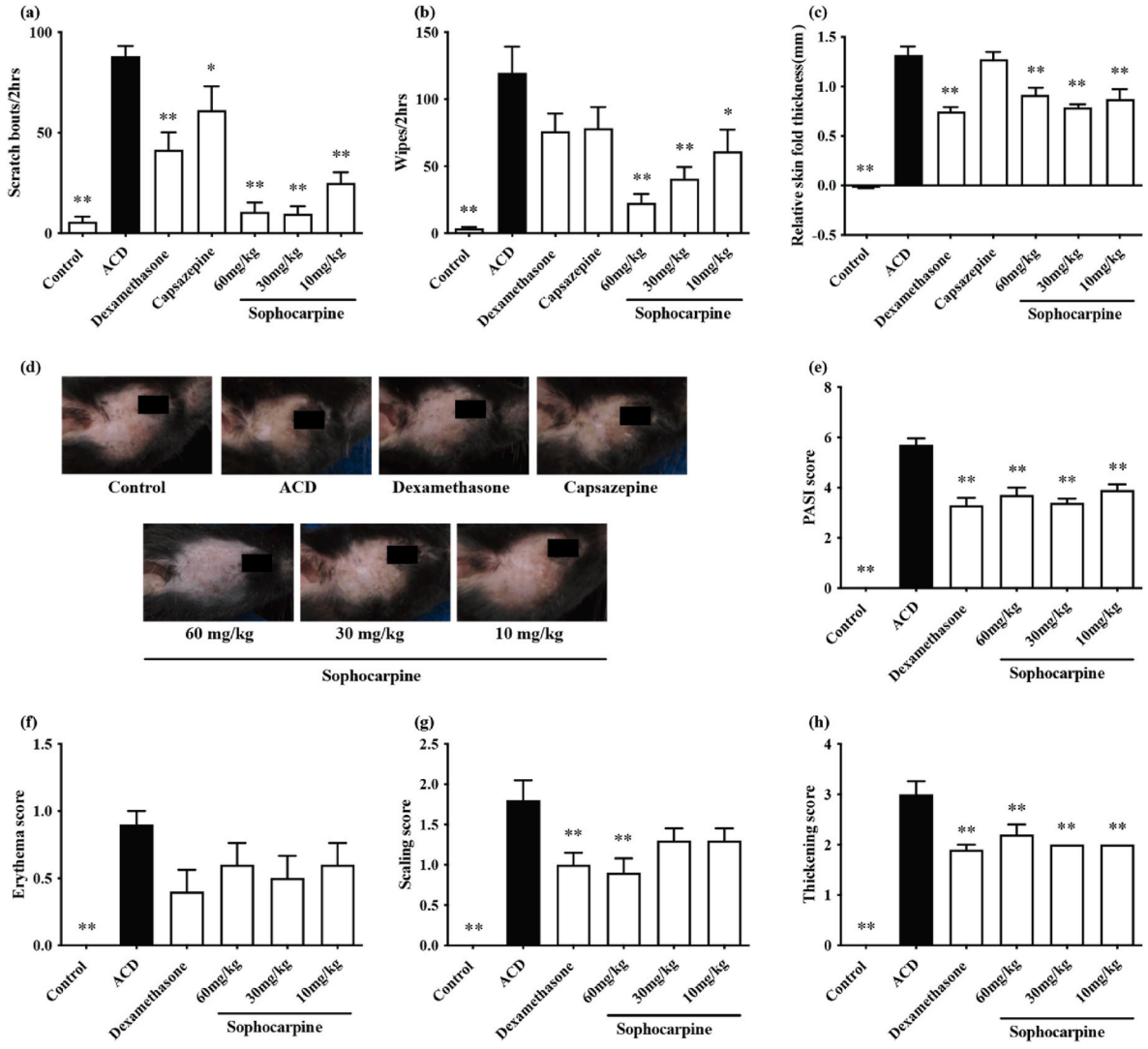

Fig. 2. Effect of sophocarpine on wiping, scratching, skinfold thickness, and severity of skin inflammation on ACD mouse model. (a) the mean of wipes; (b) the mean of scratching bouts; (c) the mean skinfold thickness differences; (d) representative photographs of the mouse cheek skin; (e) the PASI score; (f) the erythema score; (g) scaling score; (h) thickening score. The erythema, scaling, and thickening score was rated on a scale from 0 (none) to 4 (very marked), and the PASI score is calculated as the sum of the erythema, scaling, and thickening score. *$p < 0.05$, **$p < 0.01$, compared with ACD group, error bars: S.E.M. $n = 10$ mice/group.

3.3. Sophocarpine downregulated the expression of the TNF-α and IL-1β in the skin

TNF-α and IL-1β mRNA expression in mice cheek skin was significantly greater in the ACD group than in the control group (Fig. 3a and b). Dexamethasone and sophocarpine significantly downregulated SADBE-induced TNF-α and IL-1β mRNA expression (Fig. 3a and b). Significantly higher TNF-α and IL-1β protein expression were identified in the ACD group compared with the control group (Fig. 3c and d).

3.4. Sophocarpine downregulated the expression of the TRPA1 & TRPV1 in TG

TRPA1 and TRPV1 mRNA expression in TG was significantly greater in the ACD group than in the control group (Fig. 4a and b). Capsazepine and sophocarpine downregulated SADBE-induced TRPV1 and TRPA1 mRNA expression significantly. (Fig. 4a and b). Significantly higher TRPA1 and TRPV1 protein expression was identified in the ACD group compared with the control group (Fig. 4c and d). Compared with the ACD group, capsazepine had no effect, whereas sophocarpine decreased TRPA1 and TRPV1 protein expression (Fig. 4c and d).

3.5. Sophocarpine reduced scratching and wiping behavior induced by AITC and could be a competitive inhibitor of TRPA1

To determine whether sophocarpine targets TRPA1, 10 mg/kg sophocarpine was administrated intragastrically (i.g.) before treatment with AITC, the canonical TRPA1 agonist. Scratching bouts and wipes significantly increased after the AITC administration (Fig. 5a and c). The wipes peaked at 5 min after AITC and capsaicin administration, while the scratching bouts peaked at 25 min after AITC administration (Fig. 5b and d). Sophocarpine significantly decreased AITC-induced scratching bouts and wipes (Fig. 5a-d).

To further investigate the relationship between sophocarpine/AITC and TRPA1, molecular docking simulation was performed *in silico* by Autodock Vina and Chimera/ChimeraX, with the ligand of sophocarpine/AITC and HC-030031, the antagonist of TRPA1, and the receptor of TRPA1 in tetramer form. The highest binding energy estimated between HC-030031 and TRPA1 was the highest among all, while the related atomic distance of the hydrogen bond between sophocarpine and TRPA1 was the shortest among all (Table 2, Fig. 5e-g).

To further investigate the relationship among sophocarpine/AITC/HC-030031 binding to TRPA1, the competition of docking results was visualized by ChimeraX. Sophocarpine competes with AITC by binding

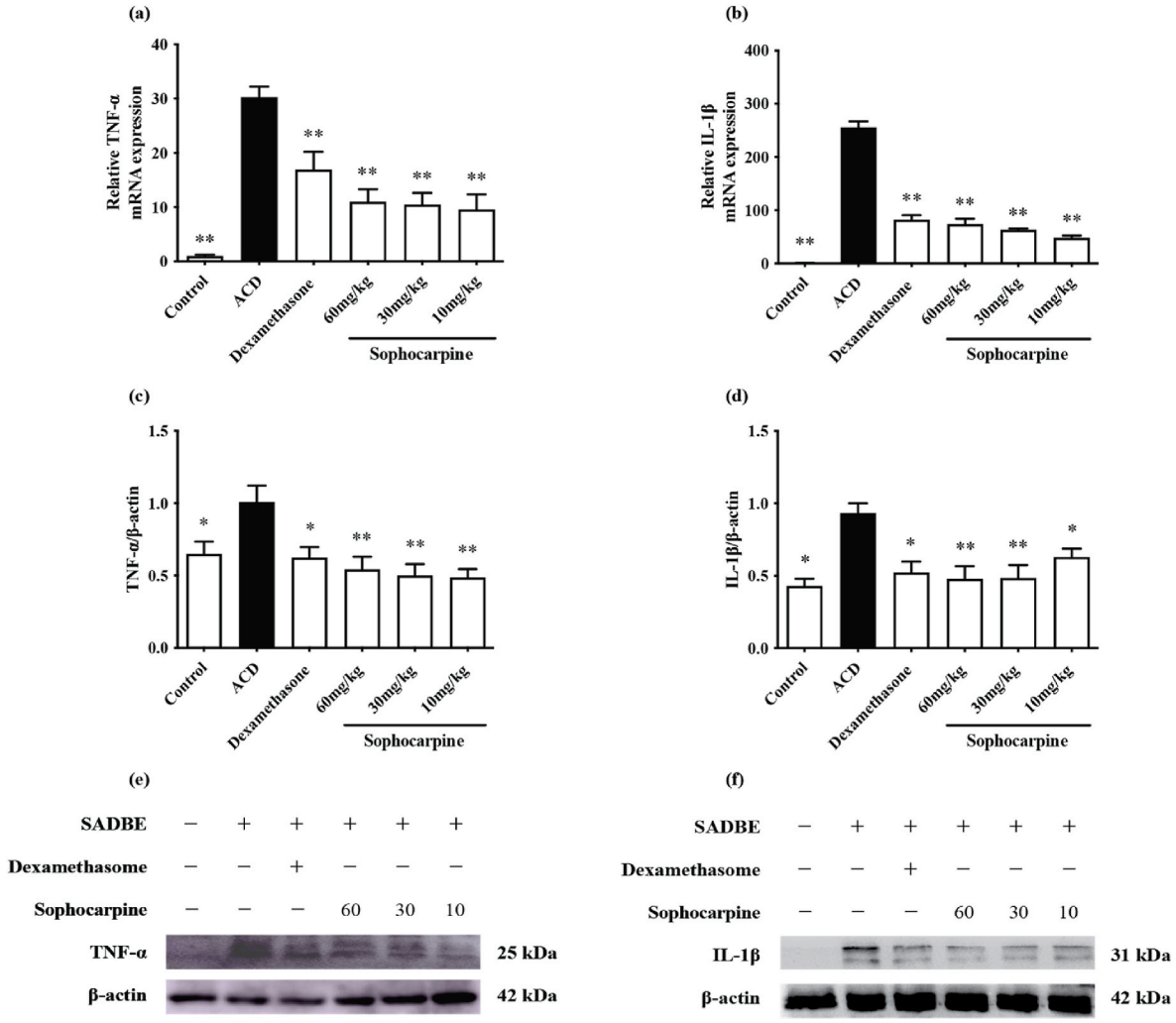

Fig. 3. Effects of sophocarpine on proinflammatory factors in the skin of ACD mouse model. (a) the mRNA expression of TNF-α; (b) the mRNA expression of IL-1β; (c) the protein expression of TNF-α; (d) the protein expression of IL-1β; (e) exemplary images of western blot of TNF-α; (f) exemplary images of western blot of IL-1β. The relative mRNA expressions were presented as 2-ΔΔCt values of the target relative to that of the β-actin. *$p < 0.05$, **$p < 0.01$ for significance compared with the ACD group, error bars: S.E.M. n = 3–6 mice/group. Representative images were cropped and adjusted for color balance and saturation by Adobe Illustrator. (For interpretation of the references to color in this figure legend, the reader is referred to the Web version of this article.)

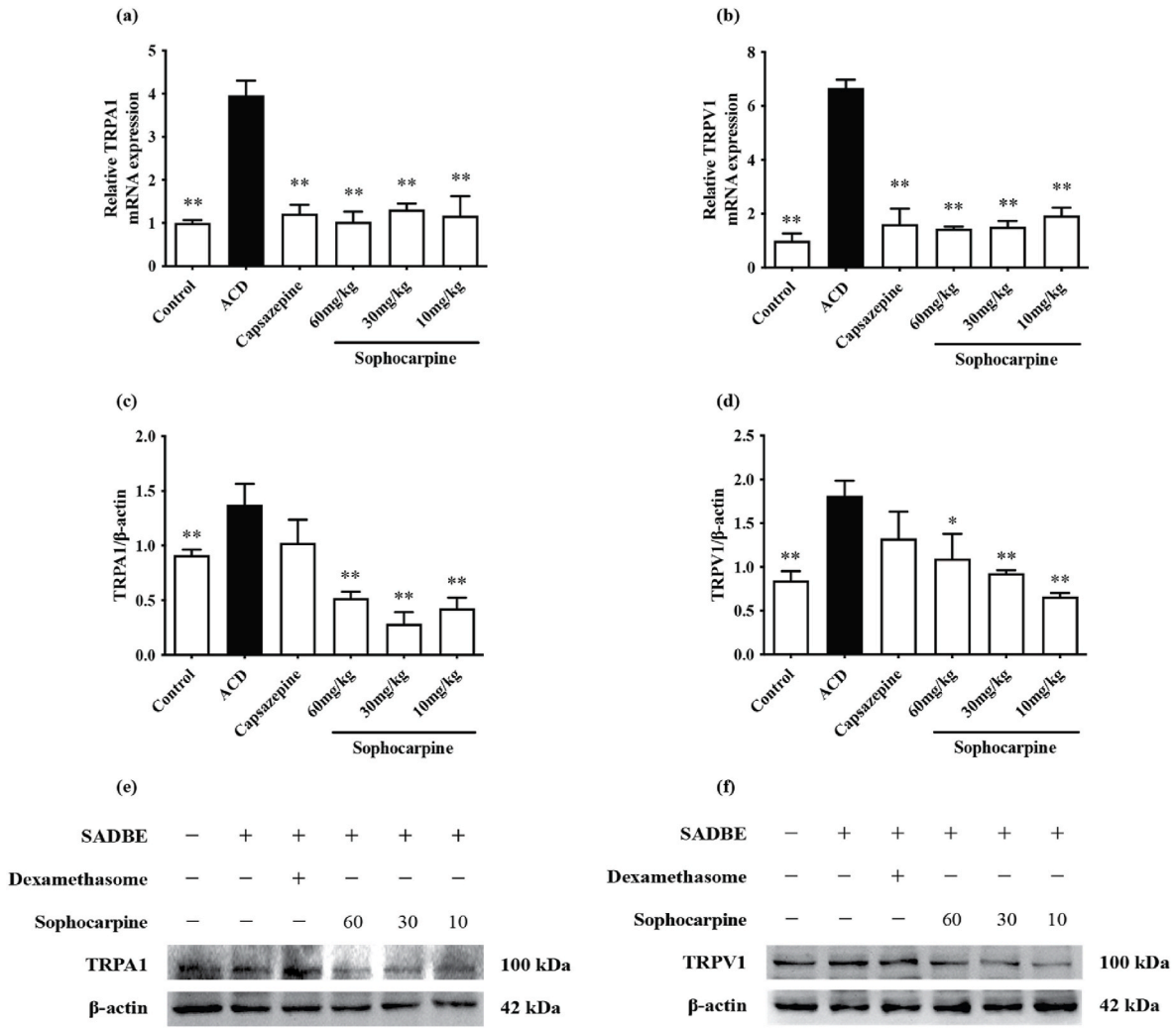

Fig. 4. Effects of sophocarpine on TRP channels expression in TG of ACD mouse model. (a) the mRNA expression of TRPA1; (b) the mRNA expression of TRPV1; (c) the protein expression of TRPA1; (d) the protein expression of TRPV1; (e) exemplary images of western blot of TRPA1; (f) exemplary images of western blot of TRPV1. The relative mRNA expressions were presented as $2^{-\Delta\Delta Ct}$ values of the target relative to that of the β-actin. $^{*}p < 0.05$, $^{**}p < 0.01$ for significance compared with the ACD group, error bars: S.E.M. n = 3–5 mice/group. Representative images were cropped and adjusted for color balance and saturation by Adobe Illustrator.

to TRPA1 monomer at the site of LYS146 in AR16, or disturbing AITC binding to ARG233, ILE234, GLU235 in the Pre-S1 helix and LEU479, SER521 in the TRP-like domain by Van der Waals, while HC-030031 competes with AITC by binding to TRPA1 monomer at the site of ARG233 in the Pre-S1 helix and SER521 in the TRP-like domain, or at the site of MET181 in AR16 and ARG233 in the Pre-S1 helix (Fig. 5h).

3.6. Sophocarpine reduced wiping behavior induced by capsaicin and could be a competitive inhibitor of TRPV1

To determine whether sophocarpine targets TRPV1, a similar treatment was performed using capsaicin instead of AITC. The wipes were significantly increased after capsaicin administration (Fig. 6c) and peaked at 5 min after capsaicin administration (Fig. 6d). Capsaicin did not induce the scratching bouts (Fig. 6a-b).

A similar method was performed to investigate the relationship between sophocarpine/capsaicin and capsazepine, the antagonist of TRPV1, and TRPV1 tetramers, and the relationship among sophocarpine/capsaicin/capsazepine when binding to TRPV1. The highest binding energy estimated between capsazepine and TRPV1 was the highest among all, while the related atomic distance of the hydrogen bond between capsaicin and TRPV1 was the shortest among all (Table 3, Fig. 6e-g). Sophocarpine competes with capsaicin by binding to the TRPV1 monomer at ARG442 in the S4-S5 linker together with the binding at SER397 in the S3, or disturbing the capsaicin binding to TRPV1 at LYS576 in the TRP domain by binding at GLU287 in the Linker domain, while capsazepine seems to compete with capsaicin only by disturbing it binding to TRPV1 by binding at ASN283 in the Linker domain (Fig. 6h).

4. Discussion

Spontaneous itch and pain are of paramount clinical relevance (Li et al., 2021). Sophocarpine was screened from SFR by our research group to bind to DRG cells (Zhang et al., 2021). Our results revealed that sophocarpine possesses strong anti-pruritic and analgesic effects, evaluated in a SADBE-induced ACD mouse model. Expression of mRNA and protein of TRPA1 and TRPV1 in sophocarpine treatment groups was decreased compared to the ACD group. Moreover, in vivo experiments showed that sophocarpine reduces AITC-induced wiping and scratching behavior and capsaicin-induced wiping behavior thus indicating that sophocarpine inhibits both TRPV1 and TRPA1 channels. Molecular docking revealed the potential of sophocarpine as a competitive inhibitor of TRPV1 and TRPA1 channels, compared with AITC and capsaicin. Therefore, we posit that sophocarpine can relieve itch and pain in ACD by downregulating expression and inhibiting the function of TRPV1 and

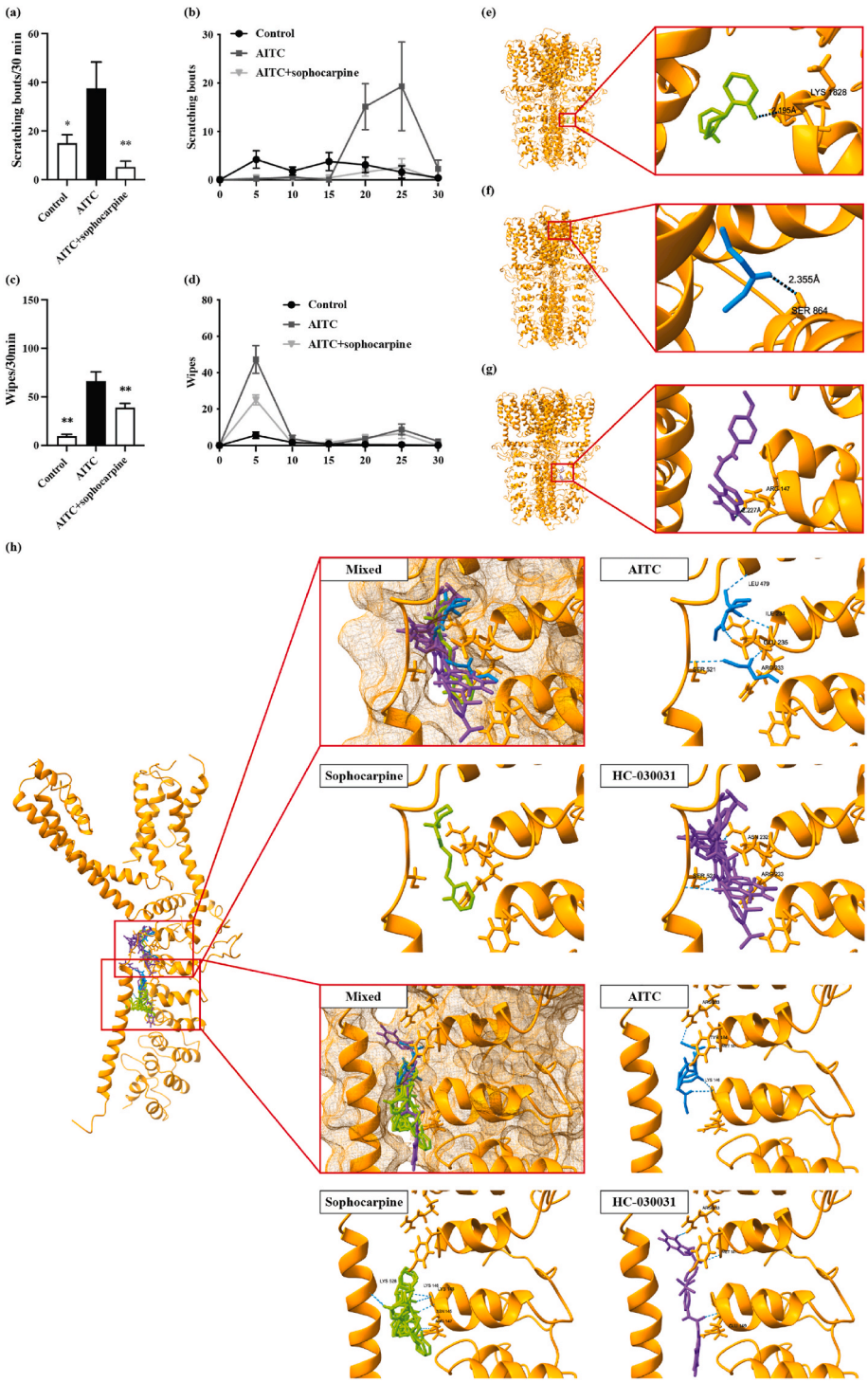

Fig. 5. Effect of sophocarpine in AITC-induced wiping and scratching behavior, and the simulation of sophocarpine binding to TRPA1 and competing with AITC. (a) the mean of scratching bouts; (b) the time course of the scratching bouts; (c) the mean of wipes; (d) the time course of the wipes; (e) the most probable simulation of sophocarpine (green) binding to TRPA1 (orange); (f) the most probable simulation of AITC (blue) binding to TRPA1 (orange); (g) the most probable simulation of HC-030031 (dark purple) binding to TRPA1 (orange); (h) two possible protein sites/pockets that sophocarpine competing with AITC binding to TRPA1 similar to HC-030031. *$p < 0.05$, **$p < 0.01$ for significance compared with AITC group, error bars: S.E.M, $n = 10$ mice/group. (For interpretation of the references to color in this figure legend, the reader is referred to the Web version of this article.)

TRPA1 channels.

The peripheral and central sensitization patterns related to chronic itch and pain are remarkably similar (Li et al., 2021). In the clinic, ACD-associated itch symptoms are presented with repeated long-lasting episodes and are sometimes accompanied by pain sensation (LaMotte, 2016). SADBE is used for the treatment of pelade and warts but causes ACD with severe itch after frequent overdosed applications, and hence SADBE is used in ACD studies (Mastrolonardo et al., 2002). Consistent with clinical observations, SADBE effectively induces ACD in mice, which display significant spontaneous scratching and wiping behavior (Qu et al., 2014). As reported previously, SADBE induces ACD in mice in this study, increasing scratching bouts and wipes significantly (Zhang

Table 2
Molecular docking simulation between ligands and TRPA1.

Ligand	Receptor	kCal/mol	Binding Type	Binding Site	Atoms Distance(Å)
Sophocarpine	TRPA1	−6.1	Hydrogen	Lys1828	2.195
AITC	TRPA1	−3.5	Hydrogen	Ser864	2.355
HC-030031	TRPA1	−8.7	Hydrogen	Arg147	2.227

et al., 2019).

SFR is widely used in relieving inflammatory itch and pain in Traditional Chinese Medicine. Oxymatrine, screened with sophocarpine from SFR by our research group, has been tested and demonstrated anti-pruritic and anti-inflammatory effects in ACD mice (Xu et al., 2018; Zhang et al., 2021). It was previously shown that sophocarpine possessed significant anti-nociceptive activity in thermally and chemically induced mouse pain models, and anti-inflammatory activity on carrageenan/xylene/acetic acid induced rat inflammation (Gao, Y. et al., 2009). In the present study, the anti-pruritic effect of sophocarpine was additionally evaluated and all effects were tested on the same mouse model. The gender difference in the ACD model has been confirmed previously (Zhang et al., 2019). Male mice were employed to avoid gender-related influence, while the result of the analgesic effect may not apply to female subjects. Our results revealed that sophocarpine significantly reduces scratching bouts and wipes in the ACD mice, thus showing a strong anti-pruritic and analgesic effect. The PASI score and skin fold thickness measurement showed that sophocarpine also treated the SADBE-induced inflammation reaction. TNF-α is the major cytokine involved in chronic inflammation inducing IL-1β and other interleukins for inflammatory signaling cascades. We also found that sophocarpine downregulated mRNA and protein expression of TNF-α and IL-1β as dexamethasone in the ACD model.

TRPA1 and TRPV1 channels are both involved in inflammatory pain and were suggested to mediate histamine-independent and histamine-dependent itch, respectively (Moore et al., 2018). SADBE could directly promote the excitability of both TRPA1 and TRPV1 channels, which is required for generating spontaneous scratching in the SADBE-induced ACD mouse models (Feng et al., 2017). In the present study, we found that TRPA1 and TRPV1 channels in trigeminal ganglia were increased after the SADBE application, consistent with previous data from the DRG.

It is suggested that the TRPA1 channel is involved in pruritus and that mice lacking the TRPA1 channel display reduced scratching and skin lesion severity, highlighting a role for TRPA1 in acute and chronic itch, and suggesting that TRPA1 antagonists may be useful for treating various pathological itch conditions (Morita et al., 2015). Nevertheless, mice lacking TRPA1 and subjected to histamine-independent itch modeling showed less reduction of scratching response to cutaneous application of borneol (Tian et al., 2023). Expression of TRPA1 channels was upregulated in patients who suffer from severe itch (Yang et al., 2015). TRPA1 also contributed to pruritus in allergic contact dermatitis (Liu et al., 2013, 2016). Nevertheless, TRPA1$^{-/-}$ mice manifest fewer pain responses when injected with bradykinin or AITC (Bautista et al., 2006). The mRNA of TRPA1 was upregulated in neuropathic pain whereas the protein of TRPA1 was increased in inflammatory pain in DRG (Caspani et al., 2009; Martínez-Rojas et al., 2021). It has been found that not ibuprofen but ibuprofen-acyl glucuronide may covalently bind to TRPA1 to reduce pain caused by AITC or other agonists (De Logu et al., 2019). Hydrogen peroxide, the side product of oxidative stress, can mediate mechanical allodynia via peripheral TRPA1 and central TRPV4, and cold hypersensitivity via mere peripheral TRPA1 (De Logu et al., 2020). A recent study on pruritus shows that protein kinase C-mediated peripheral TRPV4 phosphorylation could be one of the key processes in pruritic siganlling, implying that peripheral application of TRPV4 antagonists may be a novel alternative treatment to itch (De Logu et al., 2023).

Our results demonstrated that sophocarpine downregulates the TRPA1 expression and reduces the scratching and wiping behaviors induced by AITC, similar to TRPA1 inhibitor HC-030031 (Fischer et al., 2017). Molecular docking showed lower binding energy and a smaller atomic distance of hydrogen bond between sophocarpine and TRPA1, indicating that sophocarpine could be a potential inhibitor of TRPA1, competing with AITC. Thus, we suggest that sophocarpine efficiently inhibits the function and downregulates the expression of TRPA1 channels to relieve itch and pain in inflammatory diseases such as ACD. Molecular docking simulations demonstrated that sophocarpine completes with AITC on the intracellular AR16, the membrane Pre-S1 helix, and the TRP-like domain in the TRPA1 monomer. Although the amino acid numbers differ and the major simulations of AITC and sophocarpine demonstrated lower binding energy to the intracellular AR16 in the N-terminus, the disturbance of sophocarpine in the Pre-S1 helix and the TRP-like domain seems more convincing, compared to the simulation of DNCB and DNFB, agonists of TRPA1 to trigger itch as AITC, binding to TRPA1 in protein pockets around the Linker domain and the TRP-like domain (Wu et al., 2022). Since HC-030031 is structurally proven could inhibit TRPA1, the result of molecular docking simulation between TRPA1 and HC-030031 further potentialized the competitive inhibitor role of sophocarpine by the disturbance in the protein pockets (Gupta et al., 2016). Further studies focusing on protein pockets identified to testify whether sophocarpine is a competitive inhibitor of TRPA1 are needed.

TRPV1 channel is expressed at the highest level in the peripheral sensory neurons involved in pain perception (Caterina and Julius, 2001). The first evidence of the role of TRPV1 in peripheral pain processing arose from observations on mice injected with the TRPV1 antagonist capsazepine (Caterina et al., 2000; Davis et al., 2000). TRPV1 also contributes to acute and chronic itch conditions (Sun and Dong, 2016). Capsazepine pretreatment reduced the scratching bouts induced by the subcutaneous injection of histamine into mice's necks (Hondoh et al., 2010). The anti-pruritic and analgesic effect of capsazepine was also observed in this study in the SADBE-induced ACD mouse model. A point mutation in the coding of the S4-S5 linker in the Trpv1 gene reduced TRPV1 phosphorylation and cell membrane recruitment, successively reducing pain and histamine-dependent itch (Duo et al., 2018). Oleic acid, a natural compound, also inhibits TRPV1 to modulate itch and pain (Morales-Lázaro et al., 2016).

We showed that sophocarpine downregulated the mRNA and protein expression of TRPV1. Our behavioral tests showed that capsaicin-induced wiping was reduced by pretreatment of sophocarpine, hinting that sophocarpine could inhibit TRPV1. Thus, we suggest that sophocarpine could efficiently inhibit and downregulate the expression of TRPV1 to relieve itch and pain manifested in diseases such as ACD. Molecular docking simulations showed competitive binding energy and atomic distance of hydrogen bond between sophocarpine and TRPV1, compared with capsaicin and capsazepine, indicating that sophocarpine may be a potential competitive inhibitor of TRPV1. Molecular docking simulations also demonstrated that sophocarpine competes with capsaicin by binding to the Linker domain, the S4-S5 linker, and the S3 in the TRPV1 monomer, while capsazepine only competes with capsaicin by binding to the Linker domain. Although the amino acid numbers differ, the binding pocket around the S4-S5 linker in TRPV1 of sophocarpine competing with capsaicin simulated in this study is quite similar to the previously published simulation of capsaicin binding to TRPV1, referring to the TRPV1 structure identified (Domene et al., 2022; Liao et al., 2013). Further studies focusing on protein pockets identified to testify whether sophocarpine is a better competitive inhibitor of TRPV1 on binding at ARG442 in its S4-S5 linker are needed, compared with capsazepine which may not be a good competitive inhibitor of TRPV1.

5. Conclusions

In conclusion, sophocarpine demonstrated a strong anti-

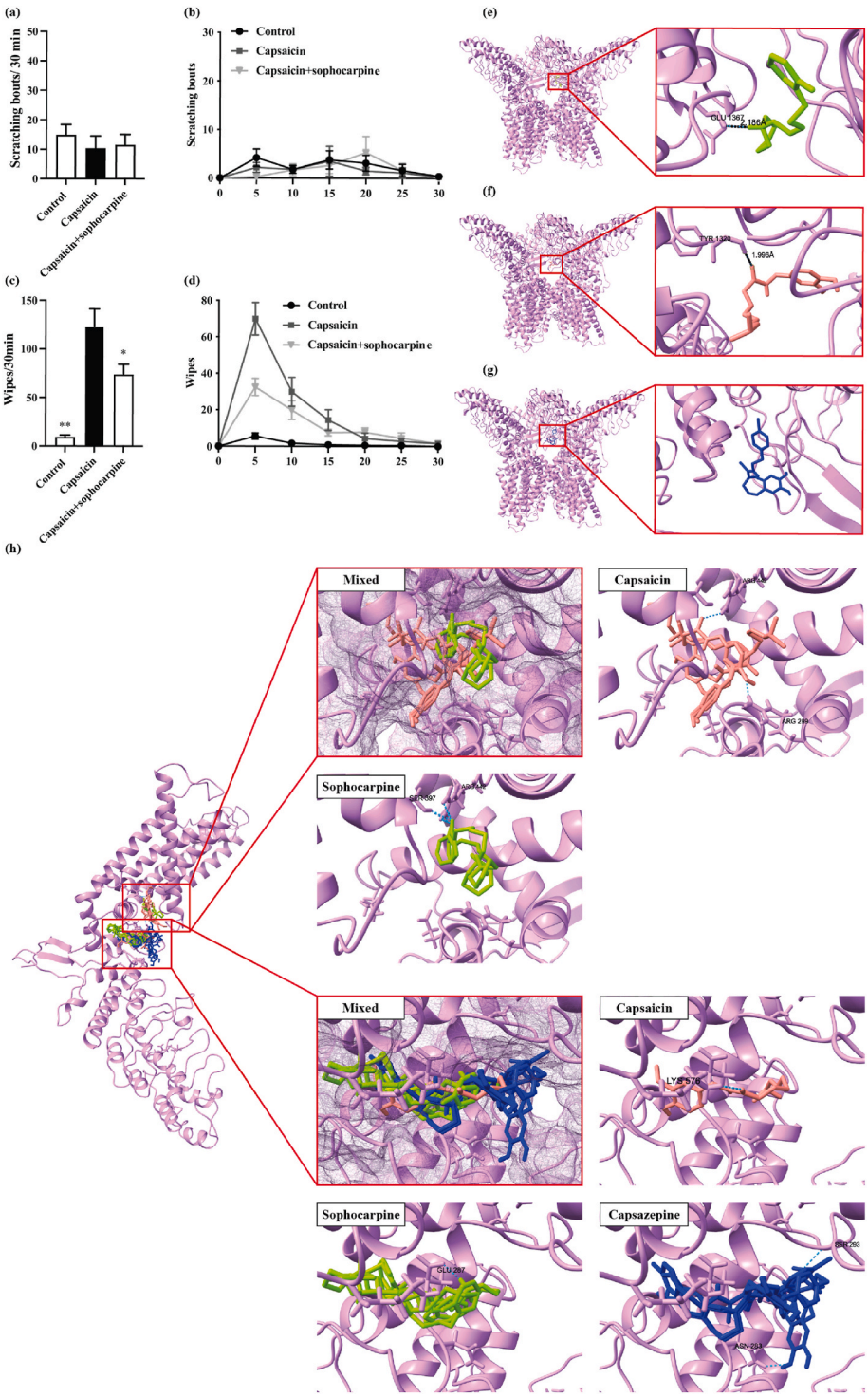

Fig. 6. Effect of sophocarpine in capsaicin-induced wiping and scratching behavior, and the simulation of sophocarpine binding to TRPV1 and competing with capsaicin. (a) the mean of scratching bouts; (b) the time course of the scratching bouts; (c) the mean of wipes; (d) the time course of the wipes; (e) the most probable simulation of sophocarpine (green) binding to TRPV1 (purple); (f) the most probable simulation of capsaicin (red) binding to TRPV1 (purple); (g) the most probable simulation of capsazepine (dark blue) binding to TRPV1 (purple); (h) two most possible protein sites/pockets that sophocarpine competing with capsaicin binding to TRPV1 similar to capsazepine. *$p < 0.05$, **$p < 0.01$ for significance compared with AITC group, error bars: S.E.M, $n = 10$ mice/group. (For interpretation of the references to color in this figure legend, the reader is referred to the Web version of this article.)

inflammatory, anti-pruritic, and analgesic effect and targeted TRP channels in TG. These findings suggest that sophocarpine might have significant therapeutic potential in treating inflammatory itch and pain.

Ethical statement

All experimental procedures and animal welfare strictly followed the Guide for the Care and Use of Laboratory Animals and related to Jinan University's ethical regulations following the Guidelines for the Ethical Review of Laboratory Animal Welfare (GB/T 35892-2018), and

Table 3
Molecular docking simulation between ligands and TRPV1.

Ligand	Receptor	kCal/mol	Binding Type	Binding Site	Atoms Distance(Å)
Sophocarpine	TRPV1	−6.4	Hydrogen	Glu1367	2.195
Capsaicin	TRPV1	−7.1	Hydrogen	Tyr1320	2.122
Capsazepine	TRPV1	−7.8	Van der Waals	N/A	N/A

approved by the Laboratory Animal Welfare and Ethics Committee of Jinan University (IACUC-20180621-07, 19 September 2023).

Fund statement

This research was funded by the National Natural Science Foundation of China (grant numbers: 81373993 & 81861138042).

CRediT authorship contribution statement

Hekun Zeng: Writing – review & editing, Writing – original draft, Visualization, Validation, Software, Investigation, Formal analysis, Data curation. **Zhe Zhang:** Writing – review & editing, Writing – original draft, Methodology, Investigation, Formal analysis. **Dan Zhou:** Writing – review & editing, Validation, Investigation. **Ranjing Wang:** Writing – review & editing, Validation, Investigation. **Alexei Verkhratsky:** Writing – review & editing, Supervision. **Hong Nie:** Writing – review & editing, Supervision, Project administration, Methodology, Funding acquisition, Conceptualization.

Declaration of competing interest

The authors declare that they have no known competing financial interests or personal relationships that could have appeared to influence the work reported in this paper.

Data availability

Data will be made available on request.

Acknowledgment

This image of *Sophorae Flavesentis* Aiton in graphic abstract was originally posted to Flickr by bastus917 at https://www.flickr.com/photos/115074382@N04/14478919164. It was reviewed on 25 June 2014 by FlickreviewR and was confirmed to be licensed under the terms of the cc-by-sa-2.0.

Abbreviations

ACD	Allergic contact dermatitis
TRP	Transient receptor potential
TRPV1	Transient receptor potential vanilloid 1
TRPA1	Transient receptor potential ankyrin 1
PASI	Psoriasis area and severity index
AITC	Allyl isothiocyanate
TNF-α	Tumor necrosis factor-α
IL-1β	Interleukin-1β
TRPC	Transient receptor potential canonical
TRPM	Transient receptor potential melastatin
TRPP	Transient receptor potential polycystin
TRPML	Transient receptor potential mucolipin
TPRN	Transient receptor potential NompC-like
SFR	Sophorae Flavesentis Radix
DRG	Dorsal root ganglion
TG	Trigeminal ganglion
SADBE	Squaric acid dibutylester
mRNA	Messenger ribonucleic acid
DNA	Deoxyribonucleic acid
cDNA	Complementary deoxyribonucleic acid
PVDF	Polyvinylidene difluoride
SDS-PAGE	Sodium dodecyl-sulfate polyacrylamide gel electrophoresis
CHS	Contact hypersensitivity
TBST	Tris-buffered saline with 0.1% Tween® 20
ANOVA	Analysis of Variance
ASN	Asparagine
LYS	Lysine
ARG	Arginine
ILE	Isoleucine
GLU	Glutamic acid
LEU	Leucine
SER	Serine
AR16	the 16th ankyrin repeat

References

Basbaum, A.I., Bautista, D.M., Scherrer, G., Julius, D., 2009. Cellular and molecular mechanisms of pain. Cell 139 (2), 267–284.

Bautista, D.M., Jordt, S.E., Nikai, T., Tsuruda, P.R., Read, A.J., Poblete, J., Yamoah, E.N., Basbaum, A.I., Julius, D., 2006. TRPA1 mediates the inflammatory actions of environmental irritants and proalgesic agents. Cell 124 (6), 1269–1282.

Burley, S.K., Bhikadiya, C., Bi, C., Bittrich, S., Chao, H., Chen, L., Craig, P.A., Crichlow, G. V., Dalenberg, K., Duarte, J.M., Dutta, S., Fayazi, M., Feng, Z., Flatt, J.W., Ganesan, S., Ghosh, S., Goodsell, D.S., Green, R.K., Guranovic, V., Henry, J., Hudson, B.P., Khokhriakov, I., Lawson, C.L., Liang, Y., Lowe, R., Peisach, E., Persikova, I., Piehl, D.W., Rose, Y., Sali, A., Segura, J., Sekharan, M., Shao, C., Vallat, B., Voigt, M., Webb, B., Westbrook, J.D., Whetstone, S., Young, J.Y., Zalevsky, A., Zardecki, C., 2023. RCSB Protein Data Bank (RCSB.org): delivery of experimentally-determined PDB structures alongside one million computed structure models of proteins from artificial intelligence/machine learning. Nucleic Acids Res. 51 (D1), D488–d508.

Caspani, O., Zurborg, S., Labuz, D., Heppenstall, P.A., 2009. The contribution of TRPM8 and TRPA1 channels to cold allodynia and neuropathic pain. PLoS One 4 (10), e7383.

Caterina, M.J., Julius, D., 2001. The vanilloid receptor: a molecular gateway to the pain pathway. Annu. Rev. Neurosci. 24, 487–517.

Caterina, M.J., Leffler, A., Malmberg, A.B., Martin, W.J., Trafton, J., Petersen-Zeitz, K.R., Koltzenburg, M., Basbaum, A.I., Julius, D., 2000. Impaired nociception and pain sensation in mice lacking the capsaicin receptor. Science 288 (5464), 306–313.

Commission, C.P., 2020. The Pharmacopoeia of the People's Republic of China, Part I, 2020 ed. China Medical Science Press, China.

Davis, J.B., Gray, J., Gunthorpe, M.J., Hatcher, J.P., Davey, P.T., Overend, P., Harries, M. H., Latcham, J., Clapham, C., Atkinson, K., Hughes, S.A., Rance, K., Grau, E., Harper, A.J., Pugh, P.L., Rogers, D.C., Bingham, S., Randall, A., Sheardown, S.A., 2000. Vanilloid receptor-1 is essential for inflammatory thermal hyperalgesia. Nature 405 (6783), 183–187.

De Logu, F., Li Puma, S., Landini, L., Tuccinardi, T., Poli, G., Preti, D., De Siena, G., Patacchini, R., Tsagareli, M.G., Geppetti, P., Nassini, R., 2019. The acyl-glucuronide metabolite of ibuprofen has analgesic and anti-inflammatory effects via the TRPA1 channel. Pharmacol. Res. 142, 127–139.

De Logu, F., Trevisan, G., Marone, I.M., Coppi, E., Padilha Dalenogare, D., Titiz, M., Marini, M., Landini, L., Souza Monteiro de Araujo, D., Li Puma, S., Materazzi, S., De Siena, G., Geppetti, P., Nassini, R., 2020. Oxidative stress mediates thalidomide-induced pain by targeting peripheral TRPA1 and central TRPV4. BMC Biol. 18 (1).

De Logu, F., Maglie, R., Titiz, M., Poli, G., Landini, L., Marini, M., Souza Monteiro de Araujo, D., De Siena, G., Montini, M., Cabrini, D.A., Otuki, M.F., Pawloski, P.L., Antiga, E., Tuccinardi, T., Calixto, J.B., Geppetti, P., Nassini, R., André, E., 2023. miRNA-203b-3p induces acute and chronic pruritus through 5-HTR2B and TRPV4. J. Invest. Dermatol. 143 (1), 142–153.e110.

Dhand, A., Aminoff, M.J., 2014. The neurology of itch. Brain 137 (Pt 2), 313–322.

Domene, C., Darré, L., Oakes, V., Gonzalez-Resines, S., 2022. A potential route of capsaicin to its binding site in the TRPV1 ion channel. J. Chem. Inf. Model. 62 (10), 2481–2489.

Duo, L., Hu, L., Tian, N., Cheng, G., Wang, H., Lin, Z., Wang, Y., Yang, Y., 2018. TRPV1 gain-of-function mutation impairs pain and itch sensations in mice. Mol. Pain 14, 1744806918762031.

Feng, J., Yang, P., Mack, M.R., Dryn, D., Luo, J., Gong, X., Liu, S., Oetjen, L.K., Zholos, A. V., Mei, Z., Yin, S., Kim, B.S., Hu, H., 2017. Sensory TRP channels contribute differentially to skin inflammation and persistent itch. Nat. Commun. 8 (1), 980.

Fischer, L., Lavoranti, M.I., de Oliveira Borges, M., Miksza, A.F., Sardi, N.F., Martynhak, B.J., Tambeli, C.H., Parada, C.A., 2017. TRPA1, substance P, histamine and 5-hydroxytryptamine interact in an interdependent way to induce nociception. Inflamm. Res. 66 (4), 311–322.

Friedman, R.M., Khalsa, P.S., Greenquist, K.W., LaMotte, R.H., 2002. Neural coding of the location and direction of a moving object by a spatially distributed population of mechanoreceptors. J. Neurosci. 22 (21), 9556–9566.

Gao, Y., Li, G., Li, C., Zhu, X., Li, M., Fu, C., Li, B., 2009. Anti-nociceptive and anti-inflammatory activity of sophocarpine. J. Ethnopharmacol. 125 (2), 324–329.
Gupta, R., Saito, S., Mori, Y., Itoh, S.G., Okumura, H., Tominaga, M., 2016. Structural basis of TRPA1 inhibition by HC-030031 utilizing species-specific differences. Sci. Rep. 6 (1).
Hondoh, A., Ishida, Y., Ugawa, S., Ueda, T., Shibata, Y., Yamada, T., Shikano, M., Murakami, S., Shimada, S., 2010. Distinct expression of cold receptors (TRPM8 and TRPA1) in the rat nodose-petrosal ganglion complex. Brain Res. 1319, 60–69.
LaMotte, R.H., 2016. Allergic contact dermatitis: a model of inflammatory itch and pain in human and mouse. Adv. Exp. Med. Biol. 904, 23–32.
Landini, L., Souza Monteiro de Araujo, D., Titiz, M., Geppetti, P., Nassini, R., De Logu, F., 2022. TRPA1 role in inflammatory disorders: what is known so far? Int. J. Mol. Sci. 23 (9).
Li, C., Kim, H.J., Back, S.K., Na, H.S., 2021. Common and discrete mechanisms underlying chronic pain and itch: peripheral and central sensitization. Pflügers Archiv 473 (10), 1603–1615.
Li, C., Niu, D., Zhu, R., Yan, X., Qu, H., Zhang, Y., Zheng, Y., 2023. Adjunctive effect of compound Kushen injection for cancer: an overview of systematic reviews. J. Ethnopharmacol. 317.
Liao, M., Cao, E., Julius, D., Cheng, Y., 2013. Structure of the TRPV1 ion channel determined by electron cryo-microscopy. Nature 504 (7478), 107–112.
Liu, B., Escalera, J., Balakrishna, S., Fan, L., Caceres, A.I., Robinson, E., Sui, A., McKay, M.C., McAlexander, M.A., Herrick, C.A., Jordt, S.E., 2013. TRPA1 controls inflammation and pruritogen responses in allergic contact dermatitis. Faseb. J. 27 (9), 3549–3563.
Liu, B., Tai, Y., Achanta, S., Kaelberer, M.M., Caceres, A.I., Shao, X., Fang, J., Jordt, S.E., 2016. IL-33/ST2 signaling excites sensory neurons and mediates itch response in a mouse model of poison ivy contact allergy. Proc. Natl. Acad. Sci. U.S.A. 113 (47), E7572–e7579.
Martínez-Rojas, V.A., Salinas-Abarca, A.B., Gómez-Víquez, N.L., Granados-Soto, V., Mercado, F., Murbartián, J., 2021. Interaction of NHE1 and TRPA1 activity in DRG neurons isolated from adult rats and its role in inflammatory nociception. Neuroscience 465, 154–165.
Mastrolonardo, M., Lopalco, P.L., Diaferio, A., 2002. Topical immunotherapy with contact sensitizers: a model to study the natural history of delayed hypersensitivity. Contact Dermatitis 47 (4), 210–214.
Miyamoto, T., Patapoutian, A., 2011. Why does morphine make you itch? Cell 147 (2), 261–262.
Moore, C., Gupta, R., Jordt, S.E., Chen, Y., Liedtke, W.B., 2018. Regulation of pain and itch by TRP channels. Neurosci. Bull. 34 (1), 120–142.
Morales-Lázaro, S.L., Llorente, I., Sierra-Ramírez, F., López-Romero, A.E., Ortíz-Rentería, M., Serrano-Flores, B., Simon, S.A., Islas, L.D., Rosenbaum, T., 2016. Inhibition of TRPV1 channels by a naturally occurring omega-9 fatty acid reduces pain and itch. Nat. Commun. 7, 13092.
Morita, T., McClain, S.P., Batia, L.M., Pellegrino, M., Wilson, S.R., Kienzler, M.A., Lyman, K., Olsen, A.S., Wong, J.F., Stucky, C.L., Brem, R.B., Bautista, D.M., 2015. HTR7 mediates serotonergic acute and chronic itch. Neuron 87 (1), 124–138.
Nilius, B., Owsianik, G., 2011. The transient receptor potential family of ion channels. Genome Biol. 12 (3), 218.
Pettersen, E.F., Goddard, T.D., Huang, C.C., Couch, G.S., Greenblatt, D.M., Meng, E.C., Ferrin, T.E., 2004. UCSF Chimera–a visualization system for exploratory research and analysis. J. Comput. Chem. 25 (13), 1605–1612.
Pettersen, E.F., Goddard, T.D., Huang, C.C., Meng, E.C., Couch, G.S., Croll, T.I., Morris, J. H., Ferrin, T.E., 2021. UCSF ChimeraX: structure visualization for researchers, educators, and developers. Protein Sci. 30 (1), 70–82.
Qu, L., Fan, N., Ma, C., Wang, T., Han, L., Fu, K., Wang, Y., Shimada, S.G., Dong, X., LaMotte, R.H., 2014. Enhanced excitability of MRGPRA3- and MRGPRD-positive nociceptors in a model of inflammatory itch and pain. Brain 137 (Pt 4), 1039–1050.
Shim, W.S., Tak, M.H., Lee, M.H., Kim, M., Kim, M., Koo, J.Y., Lee, C.H., Kim, M., Oh, U., 2007. TRPV1 mediates histamine-induced itching via the activation of phospholipase A2 and 12-lipoxygenase. J. Neurosci. 27 (9), 2331–2337.
Shimada, S.G., LaMotte, R.H., 2008. Behavioral differentiation between itch and pain in mouse. Pain 139 (3), 681–687.
Sun, S., Dong, X., 2016. Trp channels and itch. Semin. Immunopathol. 38 (3), 293–307.
Tian, W., He, D., Liu, J., Chen, F., Zhang, W., Hu, J., Wang, S., 2023. Topical borneol relieves nonhistaminergic pruritus via targeting TRPA1 and TRPM8 channels in peripheral nerve terminals of mice. Eur. J. Pharmacol. 953, 175833.
Tingle, B.I., Tang, K.G., Castanon, M., Gutierrez, J.J., Khurelbaatar, M., Dandarchuluun, C., Moroz, Y.S., Irwin, J.J., 2023. ZINC-22—A free multi-billion-scale database of tangible compounds for ligand discovery. J. Chem. Inf. Model. 63 (4), 1166–1176.
Trott, O., Olson, A.J., 2010. AutoDock Vina: improving the speed and accuracy of docking with a new scoring function, efficient optimization, and multithreading. J. Comput. Chem. 31 (2), 455–461.
Tsagareli, M.G., Nozadze, I., 2020. An overview on transient receptor potential channels superfamily. Behav. Pharmacol. 31 (5), 413–434.
Wang, J., Li, H., Yang, Z., Huang, C., Sun, Y., Hu, X., 2023. Elucidation of the Mechanisms and Molecular Targets of Run-Zao-Zhiyang.
Wilson, S.R., Gerhold, K.A., Bifolck-Fisher, A., Liu, Q., Patel, K.N., Dong, X., Bautista, D. M., 2011. TRPA1 is required for histamine-independent, Mas-related G protein-coupled receptor-mediated itch. Nat. Neurosci. 14 (5), 595–602.
Wu, H., Niu, C., Qu, Y., Sun, X., Wang, K., 2022. Selective activation of TRPA1 ion channels by nitrobenzene skin sensitizers DNFB and DNCB. J. Biol. Chem. 298 (2), 101555.
Xu, X., Xiao, W., Zhang, Z., Pan, J., Yan, Y., Zhu, T., Tang, D., Ye, K., Paranjpe, M., Qu, L., Nie, H., 2018. Anti-pruritic and anti-inflammatory effects of oxymatrine in a mouse model of allergic contact dermatitis. J. Dermatol. Sci. 91 (2), 134–141.
Yamaguchi, J., Aihara, M., Kobayashi, Y., Kambara, T., Ikezawa, Z., 2009. Quantitative analysis of nerve growth factor (NGF) in the atopic dermatitis and psoriasis horny layer and effect of treatment on NGF in atopic dermatitis. J. Dermatol. Sci. 53 (1), 48–54.
Yang, Y.S., Cho, S.I., Choi, M.G., Choi, Y.H., Kwak, I.S., Park, C.W., Kim, H.O., 2015. Increased expression of three types of transient receptor potential channels (TRPA1, TRPV4 and TRPV3) in burn scars with post-burn pruritus. Acta Derm. Venereol. 95 (1), 20–24.
Zhang, Z., Malewicz, N.M., Xu, X., Pan, J., Kumowski, N., Zhu, T., Shimada, S.G., Nie, H., LaMotte, R.H., 2019. Differences in itch and pain behaviors accompanying the irritant and allergic contact dermatitis produced by a contact allergen in mice. Pain Rep 4 (5), e781.
Zhang, Z., Pan, J., Zhu, T., Malewicz, N., Ye, K., Rong, J., Luo, Y., Situ, Y., Verkhratsky, A., Wang, Y., Zhao, J., Tang, D., Nie, H., 2021. Oxymatrine screened from Sophora flavescens by cell membrane immobilized chromatography relieves histamine-independent itch. J. Pharm. Pharmacol. 73 (12), 1617–1629.